Cellular Physiology and Biochemistry

Cell Physiol Biochem 2018;47:2216-2232
DOI: 10.1159/000491534
Published online: July 05, 2018
Accepted: April 19, 2018

Original Paper

A Preliminary Investigation of PVT1 on the Effect and Mechanisms of Hepatocellular Carcinoma: Evidence from Clinical Data, a Meta-Analysis of 840 Cases, and *In Vivo* Validation

Yu Zhang[a] Dong-yue Wen[b] Rui Zhang[a] Jia-cheng Huang[a] Peng Lin[b] Fang-Hui Ren[a] Xiao Wang[c] Yun He[b] Hong Yang[b] Gang Chen[a] Dian-Zhong Luo[a]

[a]Department of Pathology, First Affiliated Hospital of Guangxi Medical University, Nanning, [b]Department of Medical Ultrasonics, First Affiliated Hospital of Guangxi Medical University, Nanning, [c]Department of Orthopedics, Shandong Provincial Hospital affiliated to Shandong University, Jinan, China

Key Words
Pvt1 • Hepatocellular carcinoma • TCGA • GEO • CAM • MiR-424-5p • INCENP

Abstract
Background/Aims: Hepatocellular carcinoma (HCC) remains a difficult problem that significantly affects the survival of the afflicted patients. Accumulating evidence has demonstrated the functions of long non-coding RNA (lncRNA) in HCC. In the present study, we aimed to explore the potential roles of *PVT1* in the tumorigenesis and progression of HCC. ***Methods:*** In this study, quantitative reverse transcription–polymerase chain reaction (RT-qPCR) was applied to detect the differences between *PVT1* expression in HCC tissues and cell lines. Then, the Cancer Genome Atlas (TCGA) and Gene Expression Omnibus (GEO) databases were searched to confirm the relationship between PVT1 expression and HCC. Moreover, a meta-analysis comprising TCGA, GEO, and RT-qPCR was applied to estimate the expression of *PVT1* in HCC. Then, cell proliferation was evaluated *in vitro*. A chicken chorioallantoic membrane (CAM) model of HCC was constructed to measure the effect on tumorigenicity *in vivo*. To further explore the sponge microRNA (miRNA) of *PVT1* in HCC, we used TCGA, GEO, a gene microarray, and target prediction algorithms. TCGA and GEO and the gene microarray were used to select the differentially expressed miRNAs, and the different target prediction algorithms were applied to predict the target miRNAs of *PVT1*. ***Results:*** We found that *PVT1* was markedly overexpressed in HCC tissue than in normal liver tissues based on both RT-qPCR and data from TCGA, and the overexpression of *PVT1* was closely related to the gender and race of the patient as well as to higher HCC tumor grades. Also, a meta-analysis of 840

Y. Zhang and D.-y. Wen contributely equally to this work.

Gang Chen
and Hong Yang

Department of Pathology and Medical Ultrasonics, First Affiliated Hospital of Guangxi Medical University, Nanning, Guangxi, Zhuang Autonomous Region 530021 (China)
Tel. 0771-5356534, E-Mail chen_gang_triones@163.com, yanghonggx@163.com

cases from multiple sources (TCGA, GEO and the results of our in-house RT-qPCR) showed that *PVT1* gained moderate value in discriminating HCC patients from normal controls, confirming the results of RT-qPCR. Additionally, the upregulation of *PVT1* could promote HCC cell proliferation *in vitro* and *vivo*. Based on the competing endogenous RNA (ceRNA) theory, the *PVT1/miR-424-5p/INCENP* axis was finally selected for further research. The *in silico* prediction revealed that there were complementary sequences between *PVT1* and *miR-424-5p* as well as between *miR-424-5p* and *INCENP*. Furthermore, a negative correlation trend was found between *miR-424-5p* and *PVT1* based on RT-qPCR, whereas a positive correlation trend was found between *PVT1* and *INCENP* based on data from TCGA. Also, *INCENP* small interfering RNA (siRNA) could significantly inhibit cell proliferation and viability. ***Conclusions:*** We hypothesized that *PVT1* could affect the biological function of HCC cells via targeting *miR-424-5p* and regulating *INCENP*. Focusing on the new insight of the *PVT1/miR-424-5p/INCENP* axis, this study provides a novel perspective for HCC therapeutic strategies.

Introduction

Hepatocellular carcinoma (HCC) represents one of the most widespread malignancies, with extremely high rates of cancer-related deaths [1]. The majority cases are clustered in Asia and Africa, and half of these incidences and deaths have occurred in China due to chronic hepatitis B infections [1]. Though the most curative treatment is surgery, including tumor resection and liver transplantation, the high rates of postoperative recurrence and mortality remain the main obstacle for the longer survival of patients with HCC [2-4]. Taking these into consideration, it is essential to elucidate the mechanism underlying HCC, which might provide novel insights into the diagnosis and treatment of HCC patients.

Long non-coding RNAs (lncRNAs) are non-protein coding transcripts with lengths longer than 200 nucleotides [5]. It has been indicated has lncRNAs could affect different cellular functions and participate in various physiological and pathological progress [6]. Accumulating evidence has shown that the ectopic expression of lncRNAs could influence the progression of HCC by modulating the self-renewal ability of liver cancer stem cells (CSCs) and other biological functions, including proliferation, apoptosis, invasion, and metastasis [7-10]. Moreover, other articles have also reported that the aberrant expression of lncRNAs might be involved in regulating the chemotherapy resistance of HCC patients [11, 12]. The lncRNA *PVT1* is located at chromosome 8q24, which is known to be a cancer-related region [13]. Moreover, *PVT1* functions as an oncogene via interacting with MYC, encoding microRNA (miRNA), and participating in DNA rearrangement [14]. Several studies have identified *PVT1* overexpression could accelerate the development of cancers and reduce the sensitivity of cancer patients to chemistry [15-20]. It has been previously shown that *PVT1* was highly expressed in HCC compared with non-tumor tissues, and its overexpression predicts recurrence by our group and other groups [21]. We had also surveyed the genetic regulatory network of *PVT1* in HCC through a gene microarray and RNA-sequecing data mining with bioinformatics method to investigate the potential mechanism of *PVT1* in HCC, and found that *DLC1* and the Hippo signaling pathway could be closely related to the function of *PVT1* in HCC [21]; however, the functions of *PVT1* in HCC remain still elusive. In the present study, we sought to explore

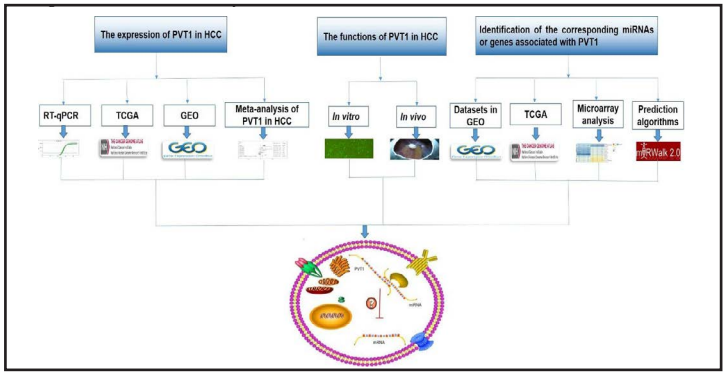

Fig. 1. A flow chart of this study.

the clinical significance, effect, and molecular mechanism of *PVT1* on the biological function of HCC cells at the cell, tissue, and animal levels. A flow chart of the current study is shown in Fig. 1.

Materials and Methods

Patient Tissue Samples

A total of 39 HCC cases from between August 2015 and January 2017 were collected from the Department of Pathology, First Affiliated Hospital of the Guangxi Medical University (Nanning, Guangxi, China). The age of these HCC patients ranged from 34 to 80 years. All patients were chosen randomly from a pool of cases who had received surgical resection without further treatment. All methods applied were according to the relevant regulations and guidelines, all experimental conventions were approved by the Ethical Committee of the First Affiliated Hospital of Guangxi Medical University, and consent forms for the use of the tissues in the study were signed by both the clinicians and patients. The pathological diagnoses were confirmed by two independent pathologists who did not know detailed patient information.

Quantitative Real-Time PCR

The total RNA was extracted via the Total RNA Kit (OMEGA, USA) based on the manufacturer's instructions. Then, the First Strand cDNA Synthesis Kit (Roche, USA) was applied to synthesize the total RNA into first-strand cDNA. The expression of *PVT1* or *miR-424-5p* was normalized to *GAPDH* or *miR-191* and *miR-103* expression. Quantitative reverse transcription–polymerase chain reaction (RT-qPCR) was performed using the FastStart Universal SYBR Green Master (ROX) (Roche) in the Applied Biosystems 7500 Real-Time PCR System. The expression level of the genes was calculated by using Delta Delta Ct method [22, 23].

The primer sequences were as follows:

- *PVT1*-forward: AAGAGAAAGGAATCGGCACA
- *PVT1*-reverse: TGGTCGGATAGGGAGTCGT
- *GAPDH*-forward: CAGCACTCTGGACGGAC
- *GAPDH*-reverse: CAACAGGAGAAGCAAACA
- *miR-424-5p*: CAGCAGCAAUUCAUGUUUUGAA
- *miR-191*: CAACGGAAUCCCAAAAGCAGCU
- *miR-103*: AGCAGCAUUGUACAGGGCUAUGA

PVT1 and HCC: A Meta-analysis

The HCC-related *PVT1* microarrays from GEO (http://www.ncbi.nlm.nih.gov/geo/) and ArrayExpress (http://www.ebi.ac.uk/arrayexpress/) were downloaded. The criteria used to determine study eligibility were as follows: 1) the study must be published in English and be a full essay; 2) it must include patients with HCC; 3) it must investigate the correlation of *PVT1* expression with HCC; 4) it must use a prospective or retrospective cohort design with a clearly defined source population and justify all excluded eligible cases; 5) false positives, false negatives, true positives, and true negatives were provided or could be calculated from the data; and 6) when the same or similar samples of patients were investigated in several publications, the latest and most complete study was selected to avoid duplication. Also, the RNA-Seq datasets in TCGA (https://cancergenome.nih.gov/) database were used, which was updated up to 30th September, 2017. Furthermore, we conducted an RT-qPCR that we included in the meta-analysis. In addition, publications related to *PVT1* in HCC were chosen from 12 online databases: PubMed, Embase, Google Scholar, Web of Science, Ovid, LILACS, Wiley Online Library, Science Direct, Chong Qing VIP, Cochrane Central Register of Controlled Trials, Wan Fang, Chinese CNKI, and China Biology Medicine disc. The retrieval was performed using the following keywords: *PVT1* AND (hepatocellular OR liver OR hepatic OR HCC) AND (malignan* OR cancer OR tumor OR tumour OR neoplas* OR carcinoma). The literature retrieval was evaluated and cross-checked by two authors (Jia-cheng Huang and Peng Lin). If there was a disagreement, the group convened and discussed.

Cell Culture and siRNA Transfection

The human HCC cell lines Bel-7402 and QGY-7703 and the normal liver cell line L02 were provided by the pathology laboratory (First Affiliated Hospital of Guangxi Medical University, China), and they were cultivated in Dulbecco's Modified Eagle's Medium (DMEM) complemented with 10% fetal bovine serum (FBS) and 1% penicillin-streptomycin. The SMMC-7721 and Bel-7404 HCC cell lines were purchased from the American Type Culture Collection (ATCC) and cultured in Roswell Park Memorial Institute (RPMI) 1640 medium supplemented with 10% FBS and 1% penicillin-streptomycin. All cells were cultured at 37°C with 5% CO_2 in a humidified incubator.

The lentiviral small interfering RNA (siRNA) vector of *PVT1* was synthesized by GeneChem (Shanghai, China; sense: 5'-CCCAACAGGAGGACAGCUUTT-3', antisense: 5'-AAGCUGUCCUCCUGUUGGGTT-3'). Both siRNA vectors that would silence the PVT1 gene and siRNA vectors that would not silence the gene were transfected into the SMMC-77221 cell line following the manufacturer's protocol.

In addition, four groups were designed to investigate the vital role of the target gene (*INCENP*) in HCC in the current study: mock control, scrambled siRNA, *INCENP* siRNA 1, and *INCENP* siRNA 2. Only the transfection reagent was added in the mock control group, whereas rearranged *INCENP* siRNA sequences were added to the scrambled siRNA group. Magnetofection (OZ Biosciences, Marseille, France) was performed for the transfection. The siRNA sequences were as follows: *INCENP* siRNA 1, 5'-GGACUUGGUGUGGCUUGAG-3'; *INCENP* siRNA 2, 5'-TGACACGGAGATTGCCAAC-3'.

Microarray Analysis

To further survey the functions of *PVT1* in HCC cells, Agilent's Human Gene Expression 4x44K Microarrays (v2) were applied to the *PVT1*-decreased SMMC-7721 cells and control cells. The Agilent Feature Extraction software (version 11.0.1.1) was utilized to obtain the original data, and the GeneSpring GX v12.1 software package (Agilent Technologies) was used to normalize and analyze the original data. We considered the genes to be significantly different when the fold change was ≥ 2 and P value was ≤ 0.05. In addition, we also conducted gene ontology (GO) and Kyoto Encyclopedia of Genes and Genomes (KEGG) pathway enrichment analyses using the GeneSpring GX v12.1 software package, which enabled us to understand the biological pathways related to the differentially expressed genes.

Identification of the Corresponding miRNAs or Genes Associated with PVT1

To further explore the corresponding miRNAs and genes associated with *PVT1*, the GEO and TCGA databases were used to further investigate the differentially expressed miRNAs or genes [24-26]. The differentially expressed miRNAs in the GEO database were chosen using the described vote-counting strategy [27]. In addition, four lncRNA/miRNA prediction algorithms were applied to predict the potential target miRNAs of *PVT1*. The four corresponding prediction algorithms were Tarbase (http://diana.imis.athena-innovation.gr/), starBase (http://starbase.sysu.edu.cn/), lncACTdb (http://210.46.85.180:8080/LncACTdb/), and TANRIC (http://ibl.mdanderson.org/tanric/_design/basic/index.html). In addition, 12 target prediction algorithms were used to predict the potential target genes of the miRNAs. The 12 corresponding prediction algorithms were DIANA microT v4 (http://diana.imis.athena-innovation.gr/), miRDB (http://www.mirdb.org/), miRWalk (http://zmf.umm.uni-heidelberg.de/apps/zmf/mirwalk2/), miRmap (http://mirmap.ezlab.org/), miRanda (http://www.microrna.org), miRBridge (http://mirsystem.cgm.ntu.edu.tw/), PicTar2 (https://www.mdc-berlin.de/), miRNAMap (http://mirnamap.mbc.nctu.edu.tw/), RNA22 (https://cm.jefferson.edu/), PITA (https://genie.weizmann.ac.il/), TargetScan (http://www.targetscan.org/), and RNAhybrid (https://bibiserv.cebitec.uni-bielefeld.de/).

In this study, the downregulated miRNAs in the GEO and TCGA databases and the miRNAs selected by the target prediction algorithms were used to identify PVT1's corresponding miRNAs. Also, the upregulated genes in the GEO and TCGA databases, the downregulated genes identified from the microarray analysis after silencing *PVT1* expression, and the genes selected by the target prediction algorithms were used to select the corresponding genes. In this process, Venn diagrams (http://bioinformatics.psb.ugent.be/webtools/Venn/) were used to identify overlapping miRNAs or genes associated with PVT1 [28, 29].

Validation of the Expression of PVT1/miRNA/mRNA

In this study, RNA-Seq data, calculated on the Illumina HiSeq RNA-Seq platform, was obtained from TCGA, including 374 HCC tissues and 50 non-tumor tissues. The expression data were exhibited as reads

per million, and the expression level was normalized via the DESeq R programming package. First, we identified the expression of *PVT1* and its relationship with the clinical pathological parameters in HCC. Then we further identified the differences in miRNA and gene expressions between HCC tissues and normal liver tissues based on TCGA. In addition, the Spearman test was performed to investigate the correlation between *PVT1* and miRNAs or genes. In addition, a receiver operating characteristic (ROC) curve was plotted to evaluate the clinical value of PVT1 expression. Furthermore, different datasets in the GEO database were used to confirm *PVT1* expression in HCC. Finally, the Human Protein Atlas (HPA, http://www.proteinatlas.org/) database was used to clarify the immunohistochemical results of genes.

Cell Proliferation

In our current study, cell proliferation was evaluated through an MTT assay. Briefly, SMMC-7721 cells were washed twice with PBS when the cell density reached 80%. The cell suspension was fabricated after being digested by trypsin, and then, cells were seeded into 96-well plates with 200 μL of volume per well, each of which containing 3×10^3–6×10^3 cells. Subsequently, MTT (20 μL, 5 mg/mL; Sigma, USA) was seeded into each well, and the cells were then incubated at 37°C with 5% CO_2 for 4 h. Dimethyl sulfoxide (DMSO; 150 μL) was placed into each well, and the cells were softly shaken for nearly 10 min to dissolve the crystal. A microplate reader was applied to distinguish the absorbance value at 490 nm at 12 h, 24 h, 48 h, 72 h, and 96 h.

Cell viability was evaluated through the fluorimetric detection of resorufin (CellTiter-Blue Cell Viability Assay, Promega, Madison, WI, USA) further confirm the results of the MTT assay. The procedure was performed based on the manufacturer's instructions. An FL600 fluorescence plate reader (Bio-Tek, Winooski, VT, USA) was applied for fluorimetry (excitation = 560 nm, emission = 590 nm). Fluorescence data were calculated as the fluorescence of treated sample/mock control×100%.

Chorioallantoic Membrane Model of HCC

Fertilized chicken eggs were purchased from a local hennery where they had been stored at 10°C and were then incubated at 37°C. Then, SMMC-7721 cells from three groups (blank group, negative control, and the *PVT1* siRNA group) were seeded into the chicken embryo chorioallantoic membrane (CAM; 2.5 × 106 cells per egg) after eight days of incubation in an incubator. Five chicken eggs were included in each group. Subsequently, the tumor growth and embryo viability were observed daily through the SZ61 Zoom Stereo Microscope (Olympus, Japan). The tumor xenografts were carefully removed from the CAMs, fixed with paraformaldehyde and embedded in paraffin after five days [30]. The size of the tumor xenografts was recorded, and the xenografts' sizes were recorded as 0 if the length of the xenograft was less than 0.2 cm.

The Potential Pathways Associated with PVT1 and miRNAs

To further investigate the fundamental functions and pathways associated with *PVT1* and miRNAs in HCC, bioinformatics analyses, including GO and KEGG analyses, were performed as described [31, 32]. Genes with more than three overlapping nucleotide sequences (either those genes listed as overexpressed in the GEO database and TCGA, shown to be downregulated in the gene microarray, or identified as the target genes of miR-424-5p by more than five prediction algorithms) were used for bioinformatics analysis. The Database for Annotation, Visualization and Integrated Discovery (DAVID; http://david.abcc.ncifcrf.gov/) was used for GO and KEGG analyses. Three independent categories (biological process [BP], cellular component [CC], and molecular function [MF]) were derived separately from the GO analysis. Also, a GO functional network was constructed via Cytoscape (v2.8, http://cytoscape.org).

Statistical Analysis

A statistical analysis was carried out using SPSS v22.0. A Student's *t*-test was conducted to discover the difference between two groups, and Kruskal–Wallis *H* test was used to estimate the relationship between three or more groups. The summary statistics between the different groups were exhibited as mean ± standard deviation (mean ± SD). A ROC curve was drawn to distinguish HCC from normal liver tissues by gene expression. Statistical significance was considered to be a *P* value was lower than 0.05 (two sides). In addition, all experiments were repeated six times.

Results

PVT1's Upregulation in HCC Tissues and Cells and Its Association with Clinical Pathological Factors

To investigate the differential expression of *PVT1* in HCC and non-cancerous liver tissue, an RT-qPCR was performed. The results showed that *PVT1* was remarkably upregulated in HCC tissues compared with the corresponding normal tissues ($P < 0.001$; Fig. 2A). Also, we conducted a ROC curve analysis to confirm the value of *PVT1* in HCC. The area under the curve (AUC) of *PVT1* was 0.857 (95% confidence interval [CI] 0.775~0.939; $P < 0.001$; Fig. 2B), and the sensitivity and specificity were 0.775 and 0.939, respectively. Furthermore, in comparison with the L02 cell line, *PVT1* was overexpressed in HCC tumor cell lines, especially SMMC-7721 ($P = 0.025$) and Bel-7404 ($P = 0.049$; Fig. 2C). In addition, to further confirm the high expression of *PVT1* in HCC tissues and its potential role in the progression of HCC, we searched TCGA for relevant tissue data, resulting in 374 HCC tissues and 50 non-tumor tissues. Compared with the corresponding normal tissues, *PVT1* was overexpressed in HCC tissues ($P < 0.001$; Fig. 2D). Moreover, the AUC of *PVT1* was 0.822 (95% CI 0.780~0.863; $P < 0.001$; Fig. 2E), and the sensitivity and specificity were 0.780 and 0.863, respectively, confirming the results of the RT-qPCR. As shown in Table 1, the expression level of *PVT1* was higher in male patients than in female patients, and it was also higher in Asian patients than in white or black patients ($P < 0.05$; Fig. 2F, 2G). Compared with the corresponding control groups, *PVT1* was also increased in HCC patients with advanced pathological grades ($P = 0.003$; Fig. 2H). Additionally, we investigated the role of *PVT1* expression in patients' survival. It was observed that patients with low *PVT1* expression survived for longer (64.31 ± 5.17 months) compared to patients with high *PVT1* expression (59.59 ± 4.75 months; $P = 0.241$; Fig. 2I). These results suggest that lncRNA *PVT1* might serve as an oncogene for HCC.

In addition, seven datasets in the GEO database (GSE54236, GSE49515, GSE60502, GSE58208, GSE98269, GSE57957, and GSE49713) were selected, and their expression data was used to evaluate *PVT1* expression. As results, we found that *PVT1* was upregulated in datasets of GSE49515, GSE58208, GSE98269, GSE57957, and GSE49713, whereas *PVT1* was downregulated in datasets of GSE54236 and GSE60502 (Table 2). The Mean ± SD of each

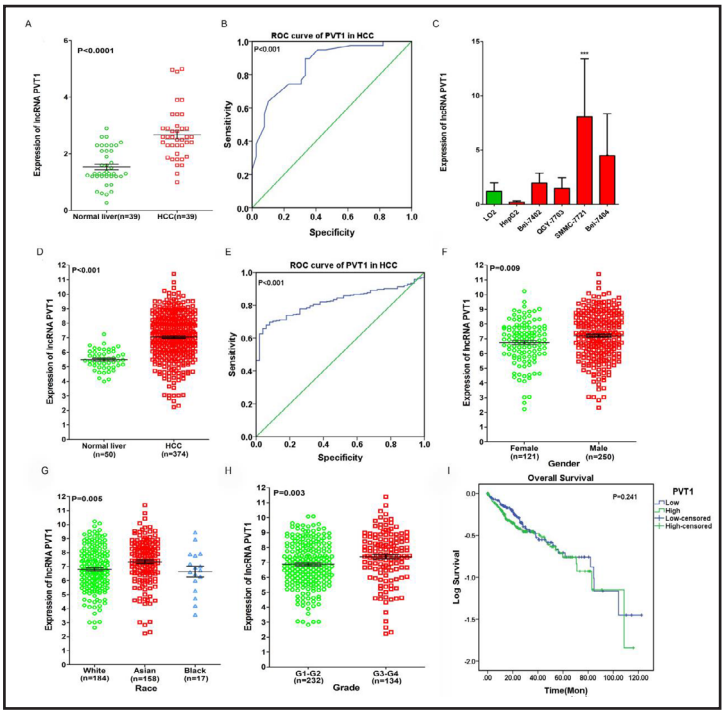

Fig. 2. Clinical significance of lncRNA PVT1 in HCC based on RT-qPCR and the Cancer Genome Atlas (TCGA) database. (A) Differential expression of PVT1 in HCC and non-cancerous liver tissue based on RT-qPCR; (B) ROC curve of PVT1 in HCC based on RT-qPCR; (C) Differential expression of PVT1 between HCC cell lines and normal liver cell line LO2 (*** P<0.001); (D) Differential expression of PVT1 between HCC and non-cancerous liver tissue based on TCGA; (E) ROC curve of PVT1 in HCC based on TCGA; (F) male vs. female; (G) White vs Yellow vs Black; (H) G1-G2 vs G3-G4; (I) Kaplan-Meier curves of PVT1 expression in HCC.

dataset was shown in Table 2.

PVT1 and HCC: A Meta-analysis of 840 Cases

After retrieving the datasets from the GEO database, 25 datasets were researched based on the keywords, and 18 datasets were excluded for not meeting our criteria. As a result, the meta-analysis included 840 cases from multiple centers (seven datasets from the GEO database [GSE54236, GSE49515, GSE60502, GSE58208, GSE98269, GSE57957 and GSE49713], the in-house RT-qPCR, and the original data in TCGA). The characteristics of these datasets included in the study are shown in Table 2. As a result, the coalescent sensitivity and specificity of *PVT1* were 0.59 (0.41–0.76) and 0.89 (0.71–0.96; Fig. 3A), respectively. The DLR negative and DLR positive were 0.46 (0.31–0.69) and 5.27 (2.05–13.52, Fig. 3B), respectively. The diagnostic score and odds ratio was 2.44 (1.38–3.51) and 11.49 (3.96–33.35; Fig. 3C), respectively. The AUC of the summary ROC (SROC) was 0.81 (0.77–0.84; Fig. 4A), which indicates that *PVT1* could be of moderate value in discriminating HCC patients from normal controls. As for the publication bias, no significant publication bias was found (P = 0.77; Fig. 4B).

As for the *PVT1* expression in the HCC group compared with the normal group, a fixed-effects model was chosen to evaluate the

Table 1. Differential expression of PVT1 by clinicopathological parameter in HCC based on TCGA

Clinicopathological parameter		N	PVT1 expression		
			Mean ± SD	T (or F value)	P value
Tissues	Normal liver	50	5.489422 ± 0.668832	12.513975	1.3668E-24
	HCC	371	7.056765 ± 1.581333		
Age	< 60	169	7.077774 ± 1.492637	0.304945	0.760580
	≥ 60	201	7.027466 ± 1.651080		
Gender	Male	250	7.205854 ± 1.624156	2.631100	0.008868
	Female	121	6.748728 ± 1.447285		
Race	White	184	6.811340 ± 1.524794	F = 5.436137	0.004726
	Asian	158	7.340178 ± 1.603716		
	Black	17	6.642498 ± 1.575141		
T (Tumor)	T1–T2	275	7.045154 ± 1.515520	-0.308312	0.758021
	T3–T4	93	7.103810 ± 1.779489		
Pathological Grade	G1–G2	232	6.874460 ± 1.490704	-2.970309	0.003172
	G3–G4	134	7.381550 ± 1.707534		
Stage	I–II	257	7.082526 ± 1.534231	0.105844	0.915768
	III–IV	90	7.061877 ± 1.750195		

Table 2. Characteristics of datasets included in the study. Note: Mean1 ± SD1 = HCC tissues, Mean0 ± SD0 = non-tumor tissues. Ref NO. The sequential reference numbers of citations. Citations of microarray datasets are displayed in the end of References list, and there are no citations available for the following 3 datasets: GSE58208[54], GSE98269[55], GSE49713[56], thus website address was affiliated

First author (publication year)	Ref NO.	Country	Data source	Test method/platform	Cancer group	Normal controls	Mean1 ± SD1	Mean0 ± SD0
Villa E et al. (2014)	[51]	Italy	GEO: GSE54236	Agilent GPL6480	81	80	7.988 ± 0.743	8.149 ± 1.036
Shi M et al. (2013)	[52]	Singapore	GEO: GSE49515	Affymetrix GPL570	10	10	3.640 ± 0.179	3.602 ± 0.049
Wang YH et al. (2014)	[53]	Chinese Taiwan	GEO: GSE60502	Affymetrix GPL96	18	18	6.512 ± 0.745	6.566 ± 0.537
Hui KM et al. (2014)	[54]	Singapore	GEO: GSE58208	Affymetrix GPL570	10	17	3.963 ± 0.122	3.855 ± 0.121
Xie Z et al. (2017)	[55]	China	GEO: GSE98269	Agilent GPL21047	3	3	6.951 ± 1.123	5.844 ± 0.087
Wang K et al. (2013)	[56]	China	GEO: GSE49713	Arraystar GPL11269	5	5	7.012 ± 0.252	6.196 ± 0.660
Mah WC et al. (2014)	[57]	Singapore	GEO: GSE57957	Illumina GPL10558	39	39	7.627 ± 0.203	7.547 ± 0.179
TCGA (2017)	NR	USA	TCGA	NR	374	50	7.044 ± 1.582	5.489 ± 0.669
RT-qPCR (2017)	NR	China	RT-qPCR	NR	39	39	2.669 ± 0.148	1.536 ± 0.104

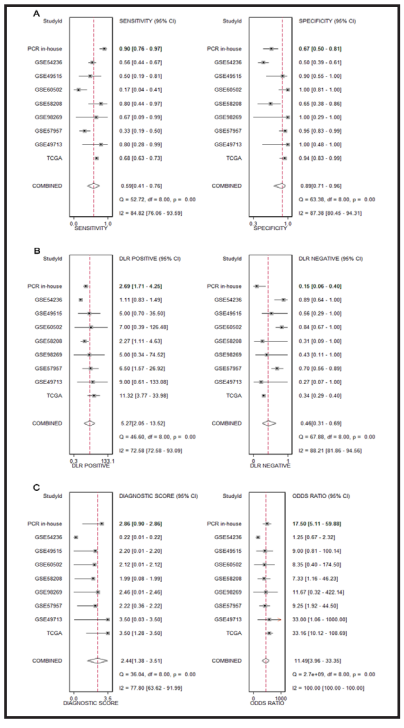

Fig. 3. Diagnostic meta-analysis of PVT1 in HCC. (A) The pooled sensitivity and specificity of the included studies, (B) the pooled positive DLR and negative DLR of the included studies, and (C) the pooled diagnostic score and diagnostic odds ratio of the included studies.

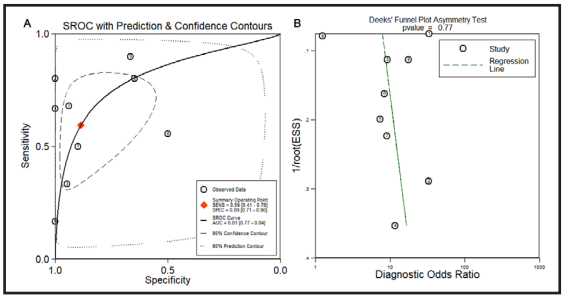

Fig. 4. Summary receiver operating characteristic (SROC) curve and publication bias of the included studies. (A) The SROC curve of PVT1 in HCC—the AUC of the SROC curve was 0.81 (0.77–0.84) (B) publication bias, where 1/root(ESS) indicates the inverse root of the effective sample sizes and each circle represents an included study.

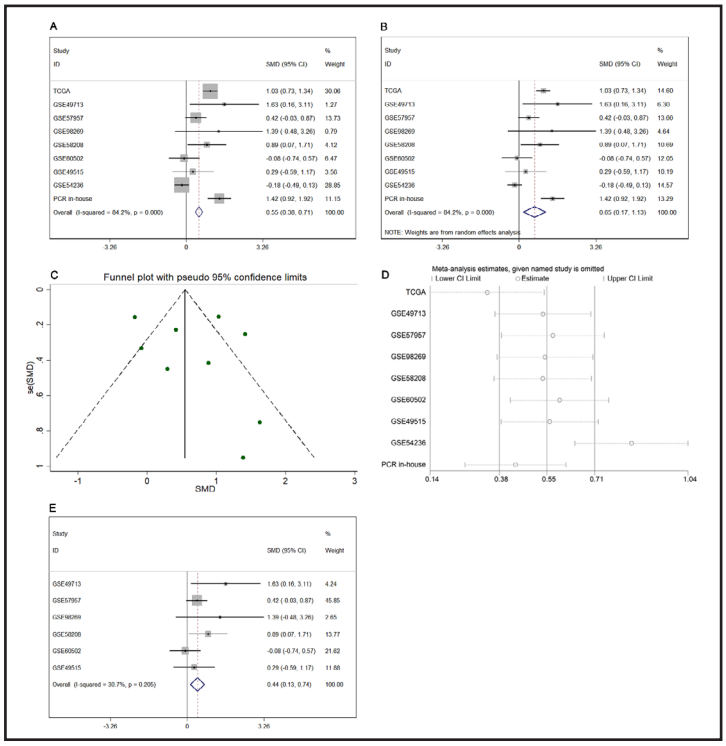

Fig. 5. Expression condition of PVT1 in HCC compared to normal liver. (A) Forest plot of datasets evaluating PVT1 expression between HCC and normal control groups (fixed-effects model); (B) forest plot of datasets evaluating PVT1 expression between HCC and normal control groups (random-effects model); (C) funnel plot of datasets, and no publication bias was found in our investigation; (D) sensitivity analysis to determine which major studies should be excluded; and (E) forest plot of the remaining datasets evaluating PVT1 expression between HCC and normal control groups (fixed-effects model).

standard mean deviation (SMD), and the combined SMD was 0.55 (0.38, 0.71) with a high heterogeneity (I^2 = 84.2%; P < 0.001; Fig. 5A). Then, a random-effects model was applied, and the combined SMD was 0.65 (0.17, 1.13) with a heterogeneity greater than 50% (Fig. 5B). As for publication bias, no significant publication bias was found (P > 0.05; Fig. 5C). In order to clarify whether a certain study contributed to the heterogeneity, a sensitivity analysis was applied to exclude two data sources (GSE54236 and the data in TCGA; Fig. 5D). Then, the fixed-effects model showed the combined SMD was 0.44 (0.13, 0.74), indicating that a higher expression of *PVT1* could be found in the HCC group than in the normal groups (Fig. 5E).

In summary, the meta-analysis of *PVT1* in HCC indicated that *PVT1* was upregulated in HCC, and *PVT1* has a moderate value in discriminating HCC patients from normal controls.

A Comprehensive Analysis of the Gene Expression Profile with Knockdown of PVT1

To explore the functions of *PVT1* in the pathogenesis of HCC, we characterized a gene expression profile by silencing *PVT1* expression. The light microscope and fluorescence microscope images after transfecting HCC cells with *PVT1* RNAi are shown in Fig. 6A and Fig. 6B. The transfection efficiency was approximately 90%, and the knockdown efficiency of *PVT1* in HCC cells was over 75% as detected by RT-qPCR (Fig. 6C). Also, the expression of *PVT1* in HCC cells was remarkably decreased in the Lv-si*PVT1* group compared to the normal control group (P = 0.035) and the Lv-control group (P = 0.029; Fig. 6C). Based on a gene microarray analysis, 195 upregulated genes and 60 downregulated genes were significantly

differentially expressed in the Lv-control and *PVT1*-RNAi groups. The top 50 differentially expressed genes are shown in Fig. 6D (|log2 FC| > 1, adjusted *P* value < 0.05).

Identification of the Corresponding miRNAs Associated with PVT1

In this study, five miRNAs (*miR-139-5p*, *miR-199a-3p*, *miR-199a-5p*, *miR-29c-3p*, *miR-424-5p*) were selected as overlapping miRNAs among the downregulated miRNAs in TCGA and GEO database. After verification by four miRNA prediction algorithms (Tarbase, starbase, lncACTdb, and TANRIC), *miR-424-5p* was the only overlapping miRNA that corresponded with *PVT1* (Fig. 7A). The complementary sequences between *miR-424-5p* and *PVT1* are shown in Fig. 7B. To investigate the differential expression of *miR-424-5p* in HCC and non-cancerous liver tissue, an RT-qPCR was performed. The results show that *miR-424-5p* was

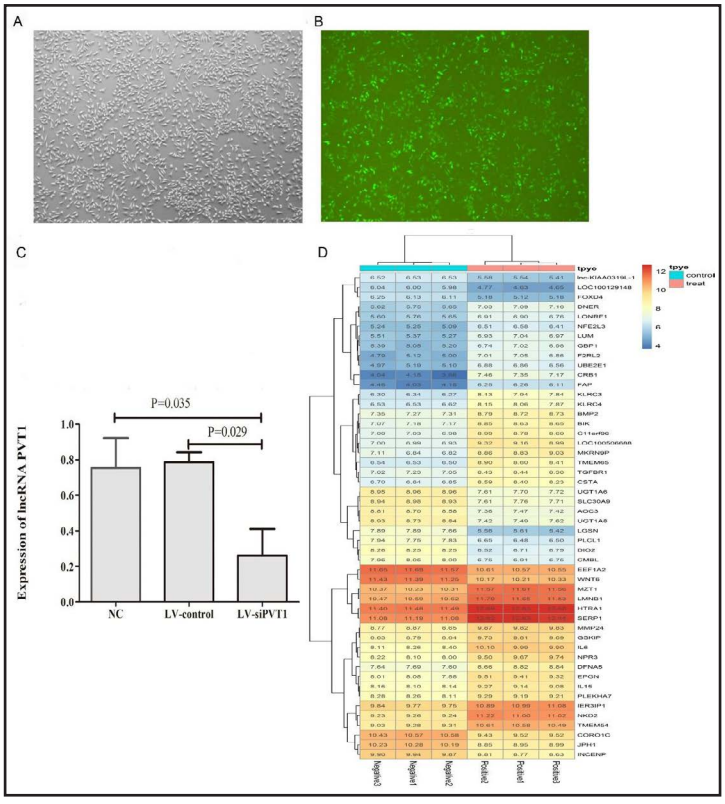

Fig. 6. Transfection efficiency of PVT1 siRNA into HCC cells. (A) Light microscope, x100; (B) fluorescence, x100; (C) the expression of PVT1 in SMMC-7721 cells was remarkably decreased in the Lv-siPVT1 group compared to the normal control group and Lv-control group based on RT-qPCR; (D) clustering heatmap visualization of genes differentially expressed among the experimental groups (n = 3) and control groups (n = 3) after PVT1 was knocked down in HCC cells. The values in the heatmap represent the levels of differentially expressed genes in each group.

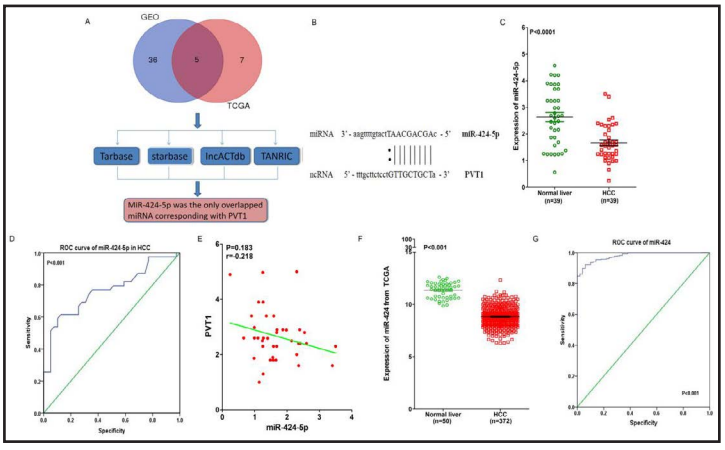

Fig. 7. Potential relationship between miR-424-5p and PVT1. (A) A flow chart to screen potential target miRNAs of PVT1; (B) Complementary sequences between miR-424-5p and PVT1; (C) The expression of miR-424-5p in HCC detected by RT-qPCR; (D) ROC curve of miR-424-5p in HCC based on RT-qPCR; (E) The relationship between the expression of miR-424-5p and PVT1 based on RT-qPCR; (F) Differential expression of miR-424 between HCC and non-cancerous liver tissue based on TCGA; (G) ROC curve of miR-424 in HCC based on TCGA.

clearly downregulated in HCC tissues compared with the corresponding non-tumor tissues ($P < 0.001$; Fig. 7C). Furthermore, a ROC curve analysis was conducted to measure the value of *miR-424-5p* in HCC. The AUC of *miR-424-5p* was 0.767 (95% CI 0.660~0.874; $P < 0.001$; Fig. 7D). Moreover, a negative correlation trend was found between *miR-424-5p* and *PVT1* (r = -0.218; P = 0.183; Fig. 7E). In addition, based on TCGA, we found that miR-424 was clearly downregulated in HCC tissues compared to normal liver tissues ($P < 0.001$; Fig. 7F). A ROC curve analysis was conducted to measure the value of miR-424 in HCC. The AUC of miR-424 was 0.978 (95% CI 0.965~0.991; $P < 0.001$; Fig. 7G). We also tried to further study the relationship between miR-424 and clinicopathological parameters based on TCGA, but no positive results were found (Table 3). Taken together, these results suggested that *PVT1* might act as a miRNA sponge in HCC by targeting *miR-424-5p*.

Identification of the Corresponding Genes Associated with PVT1

To identify the key genes associated with *PVT1* and *miR-424-5p* in HCC, only one gene expression profile (GSE57786) could be obtained from the GEO database, and the genes upregulated in GEO after *PVT1* overexpression were screened out for subsequent evaluation. TCGA was searched to select the genes overexpressed in HCC. Additionally, the 60 downregulated genes after silencing *PVT1* expression and the target genes of *miR-424-5p* predicted by more than five prediction algorithms were also considered to be candidate corresponding genes. As a result, only one gene—*INCENP*—was selected out of all the genes above via Venn diagrams (Fig. 8A). Also, the complementary sequences between *INCENP* and *miR-424-5p* are shown in Fig. 8B. Based on data from TCGA, we found that *INCENP* was clearly upregulated in HCC tissues compared to normal liver tissues ($P < 0.001$, Fig. 8C). Also, a positive correlation trend was found between *PVT1* and *INCENP* (r = 0.039, P = 0.421, Fig. 8D). Considering the relationship between *INCENP* and clinicopathological parameters, we found that high *INCENP* expression was positively related to tumor stage (P = 0.007,

Table 3. Differential expression of miR-424 by clinicopathological parameter in HCC based on TCGA

Clinicopathological parameter		N	miR-424 expression		
			Mean ± SD	T (or F value)	P value
Tissues	Normal liver	50	11.344194 ± 0.740768	-17.799339	< 0.001
	HCC	372	8.814054 ± 0.967342		
Age	< 60	170	8.842633 ± 1.015856	0.496197	0.620051
	≥ 60	201	8.792519 ± 0.928032		
Gender	Male	253	8.787174 ± 0.924067	-0.781045	0.435275
	Female	119	8.871202 ± 1.055289		
Race	White	182	8.894917 ± 0.995177	F = 1.900547	0.150996
	Asian	161	8.695467 ± 0.962687		
	Black	17	8.914114 ± 0.828981		
T (Tumor)	T1–T2	276	8.798003 ± 0.905297	-0.321656	0.748211
	T3–T4	93	8.839273 ± 1.120200		
Pathological Grade	G1–G2	231	8.839320 ± 1.013266	0.736736	0.461755
	G3–G4	137	8.762365 ± 0.888114		
Stage	I–II	258	8.792441 ± 0.909124	0.351068	0.725751
	III–IV	90	8.750941 ± 1.112777		

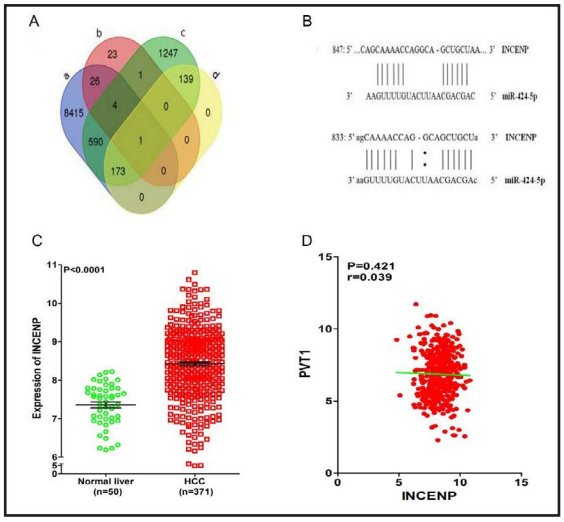

Fig. 8. Potential relationship between PVT1, miR-424-5p, and INCENP. (A) A Venn diagram to screen the possible target genes of miR-424-5p (a: the genes overexpressed in GEO, b: the downregulated genes after the knockdown of PVT1, c: the genes overexpressed in TCGA, d: target genes of miR-424-5p identified by prediction algorithms), (B) complementary sequences of miR-424-5p binding to INCENP 3'-UTR, (C) differential expression of INCENP in HCC and non-cancerous liver tissue, and (D) positive correlation between PVT1 and INCENP in TCGA.

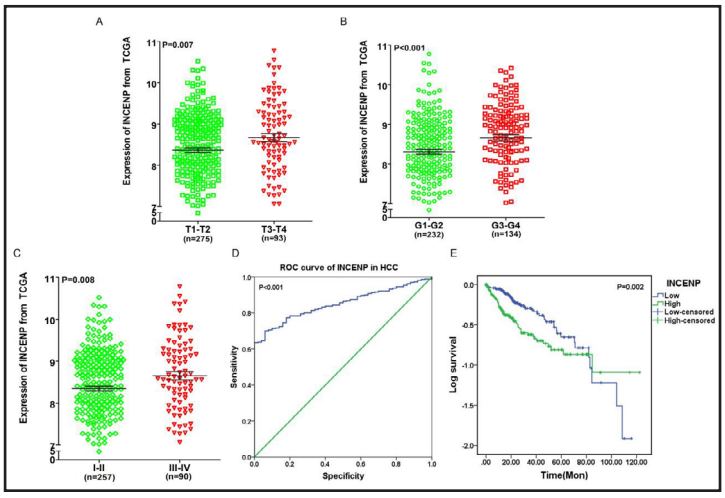

Fig. 9. Clinical significance of lncRNA INCENP in HCC based on TCGA database. (A) Differential expression of INCENP in group with TI–T2 vs. T3–T4, (B) G1–G2 vs. G3–G4, (C) stage I + II vs. stage Ⅲ + Ⅳ, (D) ROC curve of INCENP in HCC, and (E) Kaplan-Meier curves of INCENP expression in HCC.

Fig. 9A), pathological grade (P = 0.001, Fig. 9B), and clinical stage (P = 0.008, Fig. 9C, Table 4). In addition, a ROC curve was drawn to evaluate the value of *INCENP* for HCC. The AUC of *INCENP* was 0.850 (95% CI 0.812~0.889; P < 0.001; Fig. 9D). Additionally, we investigated the role of *INCENP* expression in patients' survival. It was observed that patients with low *INCENP* expression survived for longer (66.11 ± 4.55 months) compared to the high *INCENP* expression group (59.85 ± 5.36 months, P = 0.002, Fig. 9E).

Table 4. Differential expression of INCENP by other clinicopathological parameter in HCC based on TCGA

Clinicopathological parameter		N	INCENP expression		
			Mean ± SD	T (or F value)	P value
Tissues	Normal liver	50	7.328732 ± 0.542553	12.175817	4.3552E-21
	HCC	371	8.436365 ± 0.941299		
Age	< 60	169	8.537884 ± 1.000167	1.935378	0.053710
	≥ 60	201	8.348287 ± 0.883685		
Gender	Male	250	8.384874 ± 0.991803	-1.619417	0.106477
	Female	121	8.542751 ± 0.820921		
Race	White	184	8.403850 ± 0.834785	F = 0.640381	0.527698
	Asian	158	8.533994 ± 1.122029		
	Black	17	8.514034 ± 1.032755		
T (Tumor)	T1–T2	275	8.363776 ± 0.935627	-2.727720	0.006685
	T3–T4	93	8.669818 ± 0.934447		
Pathological Grade	G1–G2	232	8.304814 ± 0.919224	-3.474589	0.000573
	G3–G4	134	8.655748 ± 0.950697		
Stage	I–II	257	8.344186 ± 0.944986	-2.667586	0.008000
	III–IV	90	8.651506 ± 0.927787		

To further evaluate the proliferation of HCC cells in the four different groups (i.e., mock control, scrambled siRNA, *INCENP* siRNA 1, and *INCENP* siRNA 2.), an MTT assay and viability assay were performed to evaluate the proliferation of HCC cells. In the results of the MTT assay, HCC cells exhibited a large cell proliferation inhibition, especially in the *INCENP* siRNA groups at 72 h (P < 0.01, Fig. 10A). Consistent with the results of the MTT assay, the viability assay showed a clear inhibition of growth in the *INCENP* siRNA groups at 72 h (P < 0.01; Fig. 10B). Taken together, these results indicate that *PVT1* might contribute to the progression of HCC by modulating *INCENP*.

According to TCGA, we confirmed that INCENP expression was higher in HCC than that in normal liver tissues. Additionally, the immunohistochemical results of INCENP were

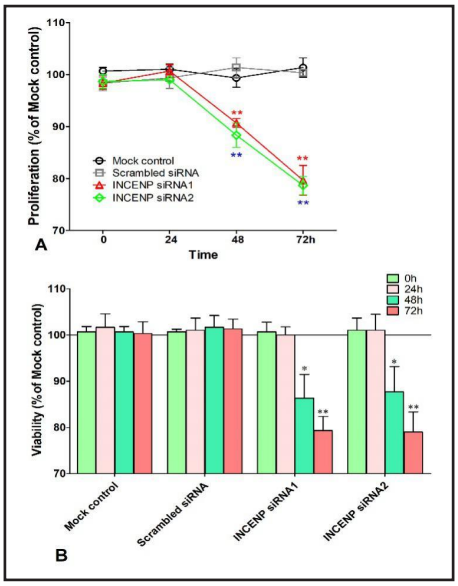

Fig. 10. Detection of the effect of INCENP on HCC cells proliferation. (A) Proliferation, (B) viability (*P<0.05, **P<0.01)

downloaded from the HPA database, which were applied to confirm INCENP expression. As shown in the HPA, INCENP could be detected in nucleus of cells. Also, INCENP was negatively stained in normal liver tissues, whereas INCENP was weakly positive stained in HCC tissues (Fig. 11). Considering the limiting samples in HPA database, no statistical analysis could be carried out. However, INCENP protein could be found in some HCC cells and none of the non-HCC cells, which was consistent with the over-expressed pattern of INCENP from TCGA data.

The Upregulation of PVT1 Promotes HCC Cell Proliferation In vitro and Vivo

To further verify the biological function of *PVT1* in HCC, we detected the cell growth capacity in HCC cells after silencing the expression of *PVT1*. The results of an MTT assay showed that Lv-si*PVT1* clearly inhibited SMCC-7721 cell proliferation at 96 h ($P < 0.05$; Fig. 12A). Furthermore, tumor formation experiments in a CAM model were conducted to evaluate the effect of *PVT1* on tumorigenesis *in vivo*. The results showed that both the lv-control and *PVT1*-RNAi group could form tumors, and the tumorigenic ability of the *PVT1*-RNAi group was significantly weakened ($P = 0.08$, Fig. 12B).

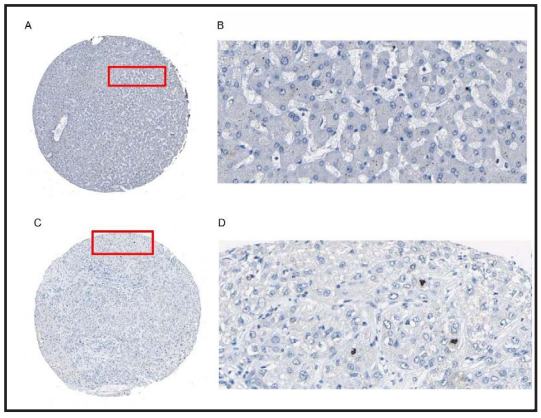

Fig. 11. The immunohistochemical results of INCENP in HCC. INCENP was negatively stained in normal liver tissues (Patient id: 3222, A, B), INCENP was weakly positive stained in HCC tissues (Patient id: 2280, C. D). These immunohistochemical results were downloaded from HPA database with the antibody of "CAB013292".

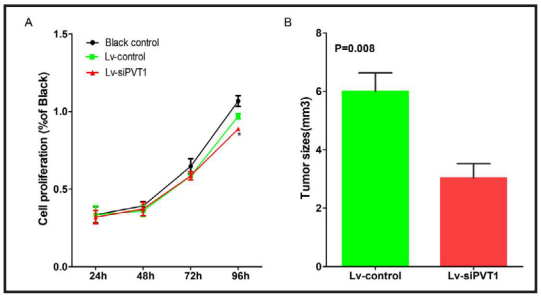

Fig. 12. Detection the effect of PVT1 on HCC growth. (A) Lv-siPVT1 inhibited the proliferation of HCC cells based on an MTT assay (*P<0.05) and (B) Comparison of the size of the HCC cell tumor xenografts after silencing PVT1 expression.

Table 5. Top 5 enrichment GO terms (BP, CC, and MF) of the 178 genes associated with PVT1 and miR-424-5p. Note: GO, gene ontology; BP, biological process; CC, cellular component; MF, molecular function

GO ID	Term	Category	Count	P value	Genes
GO:0051301	cell division	BP	14	2.09E-05	CCNF, KIF18B, BIRC5, CDC25A, CDC25B, CCNE2, CCNE1, KIF2C, NCAPH, OIP5, BUB1B, SKA3, CCNO, CDCA4
GO:0007067	mitotic nuclear division	BP	11	9.84E-05	KIF2C, OIP5, INCENP, CCNF, SKA3, BUB1B, BIRC5, ANLN, CEP55, CDC25A, CDC25B
GO:0007018	microtubule-based movement	BP	7	9.94E-05	KIF23, DYNC1I1, KIF2C, KIF24, KIF18B, RACGAP1, KIF21B
GO:0000281	mitotic cytokinesis	BP	4	0.00232	KIF23, ANLN, CEP55, RACGAP1
GO:0000082	G1/S transition of mitotic cell cycle	BP	6	0.002479	CCNE2, CCNE1, IQGAP3, MCM2, CDC25A, CDT1
GO:0005871	kinesin complex	CC	5	0.001374	KIF23, KIF2C, KIF24, KIF18B, KIF21B
GO:0005874	microtubule	CC	10	0.002236	KIF23, DYNC1I1, KIF2C, KIF24, INCENP, KIF18B, BIRC5, RACGAP1, KIF21B, EML6
GO:0000776	kinetochore	CC	5	0.006412	DYNC1I1, KIF2C, INCENP, SKA3, BUB1B
GO:0000777	condensed chromosome kinetochore	CC	5	0.008226	DYNC1I1, KIF2C, INCENP, BUB1B, BIRC5
GO:0000785	chromatin	CC	5	0.008899	OIP5, CHEK1, MCM2, HMGA1, TP73
GO:0003777	microtubule motor activity	MF	6	8.21E-04	KIF23, DYNC1I1, KIF2C, KIF24, KIF18B, KIF21B
GO:0019901	protein kinase binding	MF	10	0.007677	CCNE2, CCNE1, DBF4B, SQSTM1, EEF1A2, PFKFB2, RACGAP1, CDC25A, TP73, CDC25B
GO:0004721	phosphoprotein phosphatase activity	MF	4	0.007983	PGP, DUSP9, CDC25A, CDC25B
GO:0003682	chromatin binding	MF	10	0.009774	TICRR, TFAP2A, PYGO2, WHSC1, CBX2, PRKAA2, POLQ, LOXL2, HMGA1, TP73
GO:0005328	neurotransmitter: sodium symporter activity	MF	3	0.011495	SLC6A8, SLC6A2, SLC6A15

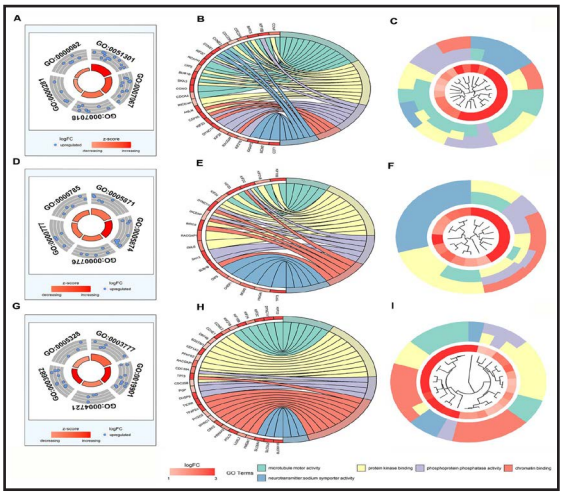

Fig. 13. Gene Ontology (GO) enrichment analysis of 178 overlapping genes. Circular visualization of gene annotation enrichment analysis. The outer circle shows a scatter plot for the logFC of the enriched genes in each GO term ([A] biological process, [D] cellular component, and [G] molecular functions). Display of the relationship between a list of enriched genes and GO terms ([B] biological process, [E] cellular component, and [H] molecular functions). Hierarchical clustering of the enriched gene expression profiles in GO terms ([C] biological process, [F] cellular component, [I] molecular functions).

The Potential Pathways Associated with PVT1 and miR-424-5p

In the current study, the GEO database, TCGA, a gene microarray, and prediction algorithms were all used to search for candidate genes, and 178 genes were selected for downstream analysis. Then, we explored the underlying gene functional pathways by GO and KEGG analyses based on these 178 genes. Consequently, cell division, protein kinase binding, as well as the kinesin complex were demonstrated to be strongly enriched biological terms that were closely associated with the progress of cancer (Table 5). To better comprehend the functions of these candidate genes, a function network was built based on the GO analysis (Fig. 13).

Table 6. KEGG pathway enrichment analysis of the 178 genes associated with PVT1 and miR-424-5p

KEGG ID	Term	Category	Count	P value	Genes
hsa04110	Cell cycle	KEGG	7	4.18E-04	CCNE2, CCNE1, BUB1B, CHEK1, MCM2, CDC25A, CDC25B
hsa04115	p53 signaling pathway	KEGG	4	0.015965	CCNE2, CCNE1, CHEK1, TP73

In addition, the KEGG pathway analysis showed that these genes were significantly overrepresented in the cell cycle and p53 signaling pathway, supporting our aforementioned result that *PVT1* might play a vital role in the proliferation of HCC cells (Table 6). Altogether, the GO and KEGG pathway items reinforced the observation that *PVT1* might be involved in HCC's biological mechanisms.

In summary, we hypothesized that *PVT1* could affect the biological function of HCC cells by targeting *miR-424-5p* and regulating *INCENP*, and the implementation of these biological functions might be involved in the p53 signaling pathway. However, various functional experiments should be conducted to verify the precise mechanism.

Discussion

lncRNAs are involved in regulating gene expression and widen our understanding of its biological functions in diseases, including cancers [33, 34]. Emerging evidence has demonstrated the functions of lncRNAs in HCC, including lncRNA-*PVT1* [7-10, 35]. As reported by xu et al., the overexpression of *PVT1* in gastric cancer can predict the poor prognosis of gastric cancer patients and promote tumor cell proliferation and invasion via binding to *FOXM1* [15]. Liu et al. also identified that *PVT1* could serve as an oncogene in prostate cancer by activating the methylation of miR-146a and thereby promoting tumor growth [16]. Another study demonstrated that *PVT1* expression was positively associated with tumor stage and metastasis, and increased expression of *PVT1* could accelerate the progression of epithelial–mesenchymal transition (EMT) in esophageal cancer cells [36]. In addition, it has also been confirmed that the inhibition of *PVT1* expression could enhance the sensitivity of cancer patients to drugs [17, 18, 37]. Despite this research, the role of PVT1 in HCC has remained elusive.

Our present study was the first to combine the analysis of data from GEO, TCGA, and gene microarrays to illustrate the biological functions of *PVT1* in HCC. In this research, we found that *PVT1* was increased in HCC tissues and cell lines, which was consistent with the results found by Ding et al. and Yu et al. [35, 38]. In addition, this study was the first to use TCGA database to show that the upregulation of *PVT1* in HCC tissues was highly associated with gender, race, and pathological grade. Ding et al.'s study demonstrated that the higher expression of *PVT1* was strongly related with AFP level and predicted poor recurrence-free survival [38]. The paper written by Yu et al. indicated that the combined upregulation of two lncRNAs (*PVT1* and *uc002mbe.2*) could provide a new method for the diagnosis of HCC, and the expression of *PVT1* and uc002mbe.2 was positively related to tumor size and clinical stage in HCC patients [33]. Furthermore, Gou et al. found that *PVT1* could promote cell proliferation and invasion in HCC by regulating *miR-214* expression [39]. Moreover, this is the first meta-analysis to survey the expression and the potential value of *PVT1* in HCC. The 0.55 SMD (0.38, 0.71) of this meta-analysis verified that HCC cells had high expressions of *PVT1*. Furthermore, in the diagnostic meta-analysis, 840 cases from GEO, TCGA, and in-house RT-qPCR were included, and the results were analyzed to estimate the validity for the detection of *PVT1* in HCC. The sensitivity of the *PVT1* assay in the included parts ranged from 41% to 76%, and the specificity ranged from 71% to 96%. The combined sensitivity (0.77) and specificity (0.84) values demonstrated the accuracy of using *PVT1* expression to detect HCC. Also, our results had an AUC of 0.81, which indicated that *PVT1* could be of moderate value in discriminating HCC patients from normal controls [40]. A PLR value of 5.27 suggested that patients with HCC had an approximately 5.27-fold higher chance of being *PVT1* assay–positive. However, there were some limitations in our meta-analysis. High heterogeneity could not be avoided partly because of blinding in the three included databases (GEO, TCGA, and in-house RT-qPCR), and we applied sensitivity analysis to exclude two data sources (GSE54236 and TCGA) to reduce heterogeneity. In addition, no adequate data from publications was found on the clinical value of *PVT1* in HCC, which may be another limitation of our meta-analysis.

In addition, SMMC-7721 cells were transfected with siRNA-*PVT1* to inhibit the expression of *PVT1*. Along with the knockdown of *PVT1*, the expression of 195 genes and 60 genes were respectively upregulated and downregulated. Then, we focused on the use of GEO, TCGA, a gene microarray and prediction algorithms, to identify *miR-424-5p* and *INCENP* as candidates for further analysis. We performed various experiments to confirm the role of *PVT1*, *miR-424-5p*, and *INCENP* in HCC. Taken the results together, we hypothesized that *PVT1* could affect the biological function of HCC cells by targeting *miR-424-5p* and regulating *INCENP*. Focusing on this new insight into the *PVT1*/*miR-424-5p*/*INCENP* axis, this study provided a novel target for the clinical prevention of and therapeutic strategy for HCC.

As previously reported, *miR-424-5p* is related to the progression of different cancers [41-44]. For example, Zhang et al. found that miR-424 was related to the pathological stage and poor prognosis of gastric cancer patients [41]. Wei et al. found that *miR-424-5p* could promote the proliferation of gastric cancer via targeting SMAD3 by the TGF-β signaling pathway [42]. Zhou et al. found that *miR-424-5p* could function as an anti-oncogene in the growth of cervical cancer cell by targeting KDM5B through the Notch signaling pathway [43]. Zhang et al. found that *miR-424-5p* was clearly downregulated in HCC tissues, and the low expression of *miR-424-5p* was critically correlated with higher pathological grades and TNM stages. Also, aberrant *miR-424-5p* expression is significantly involved in the progression of liver cancer [44]. Furthermore, growing evidence has confirmed the role of *INCENP* in cancers [45-47]. For example, Deng et al. confirmed that the methylation of *INCENP* could be involved in the growth of cancer cells [45]. Xia et al. demonstrated that the high expression of *INCENP* was associated with shorter survival in HCC patients [46]. Moreover, Adams et al. confirmed high *INCENP* levels in colon, testes, and prostate cancer cells [47]. In our current study, we verified the presence of the decreased expression of *miR-424-5p* and the overexpression of *INCENP* in HCC. Also, complementary sequences and the correlation between *PVT1*, *miR-424-5p*, and *INCENP* supported our hypothesis.

In the pathway analysis, we found that overlapping genes were significantly overrepresented in the cell cycle and the p53 signaling pathway, supporting our results that *PVT1* might play a vital role in the proliferation of HCC. The p53 signaling pathway is associated with the cell cycle, apoptosis, and poor prognosis for cancer patients [48-50]. These findings suggest that *PVT1* affects the carcinogenesis and progression of HCC by modulating the expression of *miR-424-5p* and *INCENP* through the p53 signaling pathway.

Overall, our study indicated that *PVT1* might serve as an oncogene to facilitate the progression of HCC by targeting *miR-424-5p* and regulating *INCENP*. However, the precise mechanism remains unknown, and further investigations are urgently needed.

Acknowledgements

This study was supported by the Guangxi Medical University Training Program for Distinguished Young Scholars (2017), Medical Excellence Award Funded by the Creative Research Development Grant from the First Affiliated Hospital of Guangxi Medical University and the Guangxi Science and Technology Program (Guike17195020).

Disclosure Statement

The authors declare that there are no conflict of interests.

References

1 Torre LA, Bray F, Siegel RL, Ferlay J, Lortet-Tieulent J, Jemal A: Global cancer statistics, 2012 CA Cancer J Clin 2015;65:87-108.
2 Moriguchi M, Takayama T, Higaki T, Kimura Y, Yamazaki S, Nakayama H, Ohkubo T, Aramaki O: Early cancer-related death after resection of hepatocellular carcinoma. Surgery 2012;151:232-237.
3 Guo Z, Zhong JH, Jiang JH, Zhang J, Xiang BD, Li LQ: Comparison of survival of patients with bclc stage a hepatocellular carcinoma after hepatic resection or transarterial chemoembolization: A propensity score-based analysis. Ann Surg Oncol 2014;21:3069-3076.
4 Chiche L, Menahem B, Bazille C, Bouvier V, Plard L, Saguet V, Alves A, Salame E: Recurrence of hepatocellular carcinoma in noncirrhotic liver after hepatectomy. World J Surg 2013;37:2410-2418.
5 Batista PJ, Chang HY: Long noncoding rnas: Cellular address codes in development and disease. Cell 2013;152:1298-1307.
6 Mercer TR, Dinger ME, Mattick JS: Long non-coding rnas: Insights into functions. Nat Rev Genet 2009;10:155-159.
7 Zhu P, Wang Y, Wu J, Huang G, Liu B, Ye B, Du Y, Gao G, Tian Y, He L, Fan Z: Lncbrm initiates yap1 signalling activation to drive self-renewal of liver cancer stem cells. Nat Commun 2016;7:13608.
8 Cao C, Sun J, Zhang D, Guo X, Xie L, Li X, Wu D, Liu L: The long intergenic noncoding rna ufc1, a target of microrna 34a, interacts with the mrna stabilizing protein hur to increase levels of beta-catenin in hcc cells. Gastroenterology 2015;148:415-426 e418.
9 Zhou M, Zhang XY, Yu X: Overexpression of the long non-coding rna spry4-it1 promotes tumor cell proliferation and invasion by activating ezh2 in hepatocellular carcinoma. Biomed Pharmacother 2017;85:348-354.
10 Li SP, Xu HX, Yu Y, He JD, Wang Z, Xu YJ, Wang CY, Zhang HM, Zhang RX, Zhang JJ, Yao Z, Shen ZY: Lncrna hulc enhances epithelial-mesenchymal transition to promote tumorigenesis and metastasis of hepatocellular carcinoma via the mir-200a-3p/zeb1 signaling pathway. Oncotarget 2016;7:42431-42446.
11 Jin W, Chen L, Cai X, Zhang Y, Zhang J, Ma D, Cai X, Fu T, Yu Z, Yu F, Chen G: Long non-coding rna tuc338 is functionally involved in sorafenib-sensitized hepatocarcinoma cells by targeting rasal1. Oncol Rep 2017;37:273-280.
12 Yin X, Zheng SS, Zhang L, Xie XY, Wang Y, Zhang BH, Wu W, Qiu S, Ren ZG: Identification of long noncoding rna expression profile in oxaliplatin-resistant hepatocellular carcinoma cells. Gene 2017;596:53-88.
13 Colombo T, Farina L, Macino G, Paci P: Pvt1: A rising star among oncogenic long noncoding rnas. Biomed Res Int 2015;2015:304208.

14 Cui M, You L, Ren X, Zhao W, Liao Q, Zhao Y: Long non-coding rna pvt1 and cancer. Biochem Biophys Res Commun 2016;471:10-14.
15 Xu MD, Wang Y, Weng W, Wei P, Qi P, Zhang Q, Tan C, Ni SJ, Dong L, Yang Y, Lin W, Xu Q, Huang D, Huang Z, Ma Y, Zhang W, Sheng W, Du X: A positive feedback loop of lncrna-pvt1 and foxm1 facilitates gastric cancer growth and invasion. Clin Cancer Res 2017;23:2071-2080.
16 Liu HT, Fang L, Cheng YX, Sun Q: Lncrna pvt1 regulates prostate cancer cell growth by inducing the methylation of mir-146a. Cancer Med 2016;5:3512-3519.
17 Liu E, Liu Z, Zhou Y: Carboplatin-docetaxel-induced activity against ovarian cancer is dependent on up-regulated lncrna pvt1 Int J Clin Exp Pathol 2015;8:3803-3810.
18 Zhang XW, Bu P, Liu L, Zhang XZ, Li J: Overexpression of long non-coding rna pvt1 in gastric cancer cells promotes the development of multidrug resistance. Biochem Biophys Res Commun 2015;462:227-232.
19 Liu F, Dong Q, Huang J: Overexpression of lncrna pvt1 predicts advanced clinicopathological features and serves as an unfavorable risk factor for survival of patients with gastrointestinal cancers. Cell Physiol Biochem 2017;43:1077-1089.
20 Wu D, Li Y, Zhang H, Hu X: Knockdown of lncrna pvt1 enhances radiosensitivity in non-small cell lung cancer by sponging mir-195 Cell Physiol Biochem 2017;42:2453-2466.
21 Pang C, Liu M, Fang W, Guo J, Zhang Z, Wu P, Zhang Y, Wang J: Mir-139-5p is increased in the peripheral blood of patients with prostate cancer. Cell Physiol Biochem 2016;39:1111-1117.
22 Dai J, Wu H, Zhang Y, Gao K, Hu G, Guo Y, Lin C, Li X: Negative feedback between tap63 and mir-133b mediates colorectal cancer suppression. Oncotarget 2016;7:87147-87160.
23 Wu H, Zhou J, Zeng C, Wu D, Mu Z, Chen B, Xie Y, Ye Y, Liu J: Curcumin increases exosomal tcf21 thus suppressing exosome-induced lung cancer. Oncotarget 2016;7:87081-87090.
24 Dinh TA, Vitucci EC, Wauthier E, Graham RP, Pitman WA, Oikawa T, Chen M, Silva GO, Greene KG, Torbenson MS, Reid LM, Sethupathy P: Comprehensive analysis of the cancer genome atlas reveals a unique gene and non-coding rna signature of fibrolamellar carcinoma. Sci Rep 2017;7:44653.
25 Seiler R, Black PC, Thalmann G, Stenzl A, Todenhofer T: Is the cancer genome atlas (tcga) bladder cancer cohort representative of invasive bladder cancer? Urol Oncol 2017;35:458 e451-458 e457.
26 Gao H, Wang H, Yang W: Identification of key genes and construction of microrna-mrna regulatory networks in multiple myeloma by integrated multiple geo datasets using bioinformatics analysis. Int J Hematol 2017;106:99-107.
27 Mao Y, Xu X, Wang X, Zheng X, Xie L: Is angiotensin-converting enzyme inhibitors/angiotensin receptor blockers therapy protective against prostate cancer? Oncotarget 2016;7:6765-6773.
28 Khan A, Mathelier A: Intervene: A tool for intersection and visualization of multiple gene or genomic region sets. BMC Bioinformatics 2017;18:287.
29 Zhou Y, Liao Q, Li X, Wang H, Wei F, Chen J, Yang J, Zeng Z, Guo X, Chen P, Zhang W, Tang K, Li X, Xiong W, Li G: Hyou1, regulated by lplunc1, is up-regulated in nasopharyngeal carcinoma and associated with poor prognosis. J Cancer 2016;7:367-376.
30 Xiao X, Zhou X, Ming H, Zhang J, Huang G, Zhang Z, Li P: Chick chorioallantoic membrane assay: A 3d animal model for study of human nasopharyngeal carcinoma. PloS one DOI: 10.1371/journal.pone.0130935.
31 Mirsafian H, Ripen AM, Leong WM, Chear CT, Bin Mohamad S, Merican AF: Transcriptome profiling of monocytes from xla patients revealed the innate immune function dysregulation due to the btk gene expression deficiency. Sci Rep 2017;7:6836.
32 Zhao Z, Bai J, Wu A, Wang Y, Zhang J, Wang Z, Li Y, Xu J, Li X: Co-lncrna: Investigating the lncrna combinatorial effects in go annotations and kegg pathways based on human rna-seq data. Database DOI: 10.1093/database/bav082.
33 Ponting CP, Oliver PL, Reik W: Evolution and functions of long noncoding rnas. Cell 2009;136:629-641.
34 Tsai MC, Manor O, Wan Y, Mosammaparast N, Wang JK, Lan F, Shi Y, Segal E, Chang HY: Long noncoding rna as modular scaffold of histone modification complexes. Science 2010;329:689-693.
35 Yu J, Han J, Zhang J, Li G, Liu H, Cui X, Xu Y, Li T, Liu J, Wang C: The long noncoding rnas pvt1 and uc002mbe.2 in sera provide a new supplementary method for hepatocellular carcinoma diagnosis. Medicine DOI: 10.1097/MD.0000000000004436.
36 Zheng X, Hu H, Li S: High expression of lncrna pvt1 promotes invasion by inducing epithelial-to-mesenchymal transition in esophageal cancer. Oncol Lett 2016;12:2357-2362.

37 You L, Chang D, Du HZ, Zhao YP: Genome-wide screen identifies pvt1 as a regulator of gemcitabine sensitivity in human pancreatic cancer cells. Biochem Biophys Res Commun 2011;407:1-6.
38 Ding C, Yang Z, Lv Z, Du C, Xiao H, Peng C, Cheng S, Xie H, Zhou L, Wu J, Zheng S: Long non-coding rna pvt1 is associated with tumor progression and predicts recurrence in hepatocellular carcinoma patients. Oncol Lett 2015;9:955-963.
39 Gou X, Zhao X, Wang Z: Long noncoding rna pvt1 promotes hepatocellular carcinoma progression through regulating mir-214 Cancer Biomark 2017; 20:511-519.
40 Swets JA: Measuring the accuracy of diagnostic systems. Science 1988;240:1285-1293.
41 Zhang J, Liu H, Hou L, Wang G, Zhang R, Huang Y, Chen X, Zhu J: Circular rna_larp4 inhibits cell proliferation and invasion of gastric cancer by sponging mir-424-5p and regulating lats1 expression. Mol Cancer 2017;16:151.
42 Wei S, Li Q, Li Z, Wang L, Zhang L, Xu Z: Correction: Mir-424-5p promotes proliferation of gastric cancer by targeting smad3 through tgf-beta signaling pathway. Oncotarget 2017;8:34018.
43 Zhou Y, An Q, Guo RX, Qiao YH, Li LX, Zhang XY, Zhao XL: Mir424-5p functions as an anti-oncogene in cervical cancer cell growth by targeting kdm5b via the notch signaling pathway. Life Sci 2017;171:9-15.
44 Zhang Y, Li T, Guo P, Kang J, Wei Q, Jia X, Zhao W, Huai W, Qiu Y, Sun L, Han L: Mir-424-5p reversed epithelial-mesenchymal transition of anchorage-independent hcc cells by directly targeting icat and suppressed hcc progression. Sci Rep 2014;4:6248.
45 Deng X, Von Keudell G, Suzuki T, Dohmae N, Nakakido M, Piao L, Yoshioka Y, Nakamura Y, Hamamoto R: Prmt1 promotes mitosis of cancer cells through arginine methylation of incenp. Oncotarget 2015;6:35173-35182.
46 Xia R, Chen S, Chen Y, Zhang W, Zhu R, Deng A: A chromosomal passenger complex protein signature model predicts poor prognosis for non-small-cell lung cancer. Onco Targets Ther 2015;8:721-726.
47 Adams RR, Eckley DM, Vagnarelli P, Wheatley SP, Gerloff DL, Mackay AM, Svingen PA, Kaufmann SH, Earnshaw WC: Human incenp colocalizes with the aurora-b/airk2 kinase on chromosomes and is overexpressed in tumour cells. Chromosoma 2001;110:65-74.
48 Fan M, Shen J, Liu H, Wen Z, Yang J, Yang P, Liu K, Chang Y, Duan J, Lu K: Downregulation of prrx1 via the p53-dependent signaling pathway predicts poor prognosis in hepatocellular carcinoma. Oncol Rep 2017;38:1083-1090.
49 Wang P, Cui J, Wen J, Guo Y, Zhang L and Chen X. Cisplatin induces HepG2 cell cycle arrest through targeting specific long noncoding RNAs and the p53 signaling pathway. Oncol Lett 2016; 12: 4605-4612.
50 Sun Y, Tao C, Huang X, He H, Shi H, Zhang Q, Wu H: Metformin induces apoptosis of human hepatocellular carcinoma hepg2 cells by activating an ampk/p53/mir-23a/foxa1 pathway. Onco Targets Ther 2016;9:2845-2853.
51 Villa E, Critelli R, Lei B, Marzocchi G, Camma C, Giannelli G, Pontisso P, Cabibbo G, Enea M, Colopi S, Caporali C, Pollicino T, Milosa F, Karampatou A, Todesca P, Bertolini E, Maccio L, Martinez-Chantar ML, Turola E, Del Buono M, De Maria N, Ballestri S, Schepis F, Loria P, Enrico Gerunda G, Losi L, Cillo U: Neoangiogenesis-related genes are hallmarks of fast-growing hepatocellular carcinomas and worst survival. Results from a prospective study. Gut 2016;65:861-869.
52 Shi M, Chen MS, Sekar K, Tan CK, Ooi LL, Hui KM: A blood-based three-gene signature for the non-invasive detection of early human hepatocellular carcinoma. Eur J Cancer 2014;50:928-936.
53 Wang YH, Cheng TY, Chen TY, Chang KM, Chuang VP, Kao KJ: Plasmalemmal vesicle associated protein (plvap) as a therapeutic target for treatment of hepatocellular carcinoma. BMC cancer 2014;14:815.
54 Hui KM: Gene expression profiling of PBMC from normal individuals, chronic hepatitis B carriers and hepatocellular carcinoma patients. https://www.ncbi.nlm.nih.gov/geo/query/acc.cgi?acc= GSE58208.
55 Xie Z, Wu B: Salivary lnc-PCDH9-13:1 and miR-664a-5p are Novel Hypersensitive and Specific Biomarkers in Diagnosis of Early Hepatocellular Carcinoma. https://www.ncbi.nlm.nih.gov/geo/query/acc.cgi?acc= GSE98269
56 Wang K, Guo W. The gene expression profiling array of LncRNA between tumor tissues and paired non-tumor tissues in HBV-positive hapatocellular carcinoma. https://www.ncbi.nlm.nih.gov/geo/query/acc.cgi?acc= GSE49713.
57 Mah WC, Thurnherr T, Chow PK, Chung AY, Ooi LL, Toh HC, Teh BT, Sauntharajah Y, Lee CG: Methylation profiles reveal distinct subgroup of hepatocellular carcinoma patients with poor prognosis. PloS one DOI: 10.1371/journal.pone.0104158.